

High Energy Cosmic-Rays and Neutrinos from Cosmological Gamma-Ray Burst Fireballs

Eli Waxman¹

Dept. of Condensed Matter Physics, Weizmann Institute of Science
Rehovot 76100, Israel

Abstract

The recent detection of delayed, low energy emission from Gamma-Ray Burst (GRB) sources confirmed the cosmological origin of the bursts and provided support for models where GRBs are produced by the dissipation of the kinetic energy of relativistic fireballs. In this review, ultra-high-energy, $> 10^{19}$ eV, cosmic-ray and high energy, $\sim 10^{14}$ eV, neutrino production in GRBs is discussed in the light of recent GRB and cosmic-ray observations. Emphasis is put on model predictions that can be tested with operating and planned cosmic-ray and neutrino detectors. The predicted neutrino intensity, $E_\nu^2 dN_\nu/dE_\nu \sim 3 \times 10^{-9}$ GeV/cm²s sr for $10^{14} \text{ eV} < E_\nu < 10^{16} \text{ eV}$, implies that a km² neutrino detector would observe tens of events per year correlated with GRBs, and will be able to test for neutrino properties with an accuracy many orders of magnitude better than is currently possible. The predicted production rate of high-energy protons, which is consistent with that required to account for the observed ultra-high-energy cosmic-ray (UHECR) flux, implies that operating and planned cosmic-ray detectors can test the GRB model for UHECR production. If the predicted sources are found, cosmic-ray detectors will provide us with a technique to investigate the inter-galactic magnetic field.

Invited talk presented at the Nobel Symposium *Particle Physics and The Universe*
Haga Slott, Sweden, August 1998

¹e-mail address: waxman@wicc.weizmann.ac.il

1 Introduction

The origin of Gamma-Ray Bursts (GRBs), bursts of 0.1 MeV—1 MeV photons lasting for a few seconds, remained unknown for over 20 years, primarily because GRBs were not detected until the past year at wave-bands other than γ -rays (see [1] for review of γ -ray observations). The isotropic distribution of bursts over the sky, revealed by observations of the BATSE detector on board the Compton Gamma-Ray Observatory, suggested that GRB sources lie at cosmological distances [2]. Adopting a cosmological distance scale to GRB sources, general phenomenological considerations were used to argue that the bursts are produced by the dissipation of the kinetic energy of a relativistic expanding fireball (see [3] for reviews).

The availability from the BeppoSAX satellite of accurate positions for GRBs shortly after their detection enabled during the past year the detection of GRB “afterglows,” delayed X-ray [4], optical [5] and radio [6] emission associated with GRB sources. Optical afterglow observations confirmed the cosmological origin of the bursts: Absorption lines detected in the afterglow of one burst set a lower limit $z \geq 0.835$ to its redshift [7], and the redshifts of three GRB host-galaxies were determined, GRB970508 at $z = 0.835$ [8], GRB980703 at $z = 0.965$ [9], and GRB971214 at $z = 3.42$ [10]. The characteristics of observed GRB afterglows, the existence of which has been predicted by the fireball model [11], are broadly in agreement with fireball model predictions and therefore provide strong support for the model [12]. Furthermore, the detection [6] of predicted [13] afterglow radio scintillation directly demonstrates the relativistic expansion of the source of GRB970508 [14]. It should be noted, however, that despite the general success of the fireball model the underlying sources producing GRB fireballs remain unknown.

Much like the underlying GRB source, the origin of ultra-high energy cosmic-rays (UHECRs), cosmic-rays of energy $> 10^{19}$ eV, is unknown (see [15] for a recent review). Most of the sources of cosmic-rays that have been proposed have difficulties in accelerating particles up to the highest observed energy [16, 15], which is in excess of 10^{20} eV [17, 18, 19, 20, 21]. Furthermore, since the distance traveled by the highest energy particles must be smaller, due to interaction with radiation backgrounds [22], than 100 Mpc [23], their arrival directions are inconsistent with the position of any astrophysical object that is likely to produce high energy particles [24]. Well before the recent confirmation of the hypothesis that GRBs are of cosmological origin, it has been shown that cosmological fireballs are likely sources of $> 10^{19}$ eV protons. The physical conditions in the fireball dissipation region imply that protons may be Fermi accelerated in this region to energy $> 10^{20}$ eV [25, 26]. In addition, the average rate at which energy is emitted as γ -rays by GRBs is remarkably comparable to the energy generation rate of UHECRs in a model where UHECRs are produced by a cosmological distribution of sources [25, 27]. These two facts suggest that GRBs and UHECRs have a common origin². The GRB fireball model for UHECR production makes several unique predictions [29, 30], which can be tested with operating (HiRes [31]), and planned (Auger [32], Telescope-Array [33]) UHECR detectors. Possibly the most interesting consequence of proton acceleration in GRB fireballs is the conversion of a significant fraction, $\simeq 10\%$, of the fireball energy to an accompanying

²Milgrom & Usov suggested [28] a GRB–UHECR association based on the overlap of the Fly’s Eye highest energy cosmic ray arrival direction error box with the position error box of a bright GRB. A correlation between GRB and UHECR arrival directions is not expected, as explained in §4, for cosmological GRBs.

burst of $\sim 10^{14}$ eV neutrinos [34]. The predicted flux implies detection of tens of events per year correlated with GRBs in planned km^2 neutrino detectors (AMANDA-II and DeepIce [35] extensions of the operating AMANDA detector [36], ANTARES [37], NESTOR [38]).

In this paper, high-energy cosmic-ray and neutrino production in GRBs is discussed in the light of recent GRB and ultra-high-energy cosmic-ray observations. In §2 the fireball model is briefly described, and implications of recent afterglow observations are discussed, which are of importance for high energy particle production. A more detailed discussion of GRBs and the fireball model is given in a separate contribution to these proceedings [39]. In section §3 recent UHECR observations, described in detail elsewhere in these proceedings [40], are discussed. The flux and spectrum measured by the Fly’s Eye, Yakutsk, and AGASA experiments are compared with the prediction of a model where UHECRs are protons accelerated to high energy by Fermi shock acceleration in sources which are uniformly distributed in the universe. The main spectral feature predicted by such a model is a “GZK cutoff” [22], a suppression of UHECR flux above $\sim 5 \times 10^{19}$ eV due to interaction of protons with the microwave background. We show that present data do not allow to confirm or rule out the existence of the predicted suppression. While both Fly’s Eye and Yakutsk data show a suppression at 2σ significance, a discrepancy may be emerging between this data and the results of the AGASA experiment: the Fly’s Eye experiment and the Yakutsk experiment each report one event beyond 10^{20} eV (close to the average number of 1.5 events predicted by the cosmological model), while the AGASA experiment reports 6 events for similar exposure. Much larger exposure than presently available is required to determine whether or not a GZK “cutoff” exists.

The production in GRB fireballs of UHECRs is discussed in §4. Predictions of the GRB model for UHECR production, that can be tested with future UHECR experiments, are discussed in §5. High energy neutrino production in fireballs and its implications for future high energy neutrino detectors are discussed in §6. The discussion in §4–§6 of UHECR and neutrino production in GRBs is similar to the analysis presented prior to the discovery of GRB afterglow [25, 34]. Some quantitative modifications are introduced due to the revised GRB energy scale, $\sim 10^{53}$ erg (for isotropic emission) implied by afterglow observations compared to $\sim 10^{52}$ erg previously assumed, and due to some, yet inconclusive, evidence that the local GRB rate is lower than previously estimated, $\sim 1 \text{ Gpc}^{-3}\text{yr}^{-1}$ compared to $\sim 10 \text{ Gpc}^{-3}\text{yr}^{-1}$. We also address some criticism of the GRB model of UHECR production recently made in the literature regarding the energy loss of protons escaping the fireball [41], and the acceleration process [42]. We show that this criticism is inapplicable to the model for UHECR production discussed here, which was proposed in [25]. Finally, in §7 a summary is presented of the main points discussed in the paper.

2 GRB fireballs and afterglow observations

2.1 The fireball model

General phenomenological considerations, based on γ -ray observations, indicate that, regardless of the nature of the underlying sources, GRBs are produced by the dissipation of the kinetic energy of a relativistic expanding fireball. The rapid rise time and short duration, ~ 1 ms, observed in some bursts [43] imply that the sources are compact, with a linear scale $r_0 \sim 10^7$ cm.

The high γ -ray luminosity required for cosmological bursts, $L_\gamma \sim 10^{52} \text{ erg s}^{-1}$, then results in an initially optically thick (to pair creation) plasma of photons, electrons and positrons, which expands and accelerates to relativistic velocities [44]. This is true whether the energy is released instantaneously, i.e. over a time scale r_0/c , or as a wind over a duration comparable to the entire burst duration (\sim seconds). In fact, the hardness of the observed photon spectra, which extends to ~ 100 MeV, implies that the γ -ray emitting region must be moving relativistically, with a Lorentz factor $\Gamma \sim 300$ [45], in order that the fireball pair-production optical depth be small for the observed high energy photons.

If the observed radiation is due to photons escaping the fireball/wind as it becomes optically thin, two problems arise. First, the photon spectrum is quasi-thermal, in contrast with observations. Second, the source size, $r_0 \sim 10^7 \text{ cm}$, and the total energy emitted in gamma-rays, $\sim 10^{53} \text{ erg}$, suggests that the underlying energy source is related to the gravitational collapse of $\sim 1M_\odot$ object. Thus, the plasma is expected to be “loaded” with baryons which may be injected with the radiation or present in the atmosphere surrounding the source. A small baryonic load, $\geq 10^{-8}M_\odot$, increases the optical depth (due to Thomson scattering) so that most of the radiation energy is converted to kinetic energy of the relativistically expanding baryons before the plasma becomes optically thin [46]. To overcome both problems it was proposed [47] that the observed burst is produced once the kinetic energy of the ultra-relativistic ejecta is re-randomized by some dissipation process at large radius, beyond the Thomson photosphere, and then radiated as γ -rays. Collision of the relativistic baryons with the inter-stellar medium [47], and internal collisions within the ejecta itself [48], were proposed as possible dissipation processes.

Most GRBs show variability on time scales much shorter than (typically one hundredth of) the total GRB duration. Such variability is hard to explain in models where the energy dissipation is due to external shocks [49, 50]. Thus, it is believed that internal collisions are responsible for the emission of gamma-rays. At small radius, the fireball bulk Lorentz factor, Γ , grows linearly with radius, until most of the wind energy is converted to kinetic energy and Γ saturates at $\Gamma \sim 300$. Variability of the source on time scale Δt , resulting in fluctuations in the wind bulk Lorentz factor Γ on similar time scale, then leads to internal shocks in the expanding fireball at a radius

$$r_i \approx \Gamma^2 c \Delta t = 3 \times 10^{13} \Gamma_{300}^2 \Delta t_{10\text{ms}} \text{ cm}, \quad (1)$$

where $\Gamma = 300\Gamma_{300}$, $\Delta t = 10\Delta t_{10\text{ms}}$ ms. If the Lorentz factor variability within the wind is significant, internal shocks would reconvert a substantial part of the kinetic energy to internal energy. It is assumed that this energy is then radiated as γ -rays by synchrotron and inverse-Compton emission of shock-accelerated electrons. For internal collisions, the observed gamma-ray variability time, $\sim r_i/\Gamma^2 c \approx \Delta t$, reflects the variability time of the underlying source, and the GRB duration reflects the duration over which energy is emitted from the source. Since the wind Lorentz factor is expected to fluctuate on time scales ranging from the shortest variability time Δt to the wind duration T , internal collisions will take place over a range of radii, $r \sim r_i = \Gamma^2 c \Delta t$ to $r \sim \Gamma^2 c T$. A large fraction of bursts detected by BATSE show variability on the shortest resolved time scale, ~ 10 ms. Our choice in Eq. (1) of $\Delta t = 10$ ms as a representative value is therefore conservative, in the sense that the shortest variability time may be significantly smaller. In fact, recent analysis indicates that variability on ~ 1 ms is

common [51].

Internal shocks are expected to be “mildly” relativistic in the fireball rest frame [48], i.e. characterized by Lorentz factor $\gamma_i - 1 \sim 1$ (since adjacent shells within the wind are expected to expand with Lorentz factors which do not differ by more than an order of magnitude). The internal shocks would therefore heat the protons to random velocities (in the wind frame) $\gamma_p - 1 \sim 1$. The characteristic frequency of synchrotron emission is determined by the characteristic energy of the electrons and by the strength of the magnetic field. These are determined by assuming that the fraction of energy carried by electrons is ξ_e , implying a characteristic rest frame electron Lorentz factor $\gamma_e = \xi_e(m_p/m_e)$, and that a fraction ξ_B of the energy is carried by the magnetic field, implying $4\pi r_i^2 c \Gamma^2 B^2 / 8\pi = \xi_B L$ where L is the total wind luminosity. Since the electron synchrotron cooling time is short compared to the wind expansion time, electrons lose their energy radiatively and $L \approx L_\gamma / \xi_e$. The characteristic observed energy of synchrotron photons, $E_\gamma = \Gamma \hbar \gamma_e^2 e B / m_e c$, is therefore

$$E_\gamma \approx 0.1 (\xi_B / 0.3)^{1/2} (\xi_e / 0.3)^{3/2} \frac{L_{\gamma,52}^{1/2}}{\Gamma_{300}^2 \Delta t_{10\text{ms}}} \text{ MeV}, \quad (2)$$

where $L_\gamma = 10^{52} L_{\gamma,52} \text{ erg/s}$. At present, there is no theory that allows the determination of the values of the equipartition fractions ξ_e and ξ_B . However, it is encouraging that for values close to equipartition, the photon energy predicted by the model is similar to that observed.

As the fireball expands, it drives a relativistic shock (blastwave) into the surrounding gas, e.g. into the inter-stellar medium (ISM) gas if the explosion occurs within a galaxy. In what follows, we refer to the surrounding gas as “ISM gas,” although the gas need not necessarily be inter-stellar. At early time, the fireball is little affected by the interaction with the ISM. At late time, most of the fireball energy is transferred to the ISM, and the flow approaches the self-similar blast-wave solution of Blandford & McKee [52]. At this stage a single shock propagates into the ISM, behind which the gas expands with Lorentz factor

$$\Gamma_{BM}(r) = 150 \left(\frac{E_{53}}{n_1} \right)^{1/2} r_{17}^{-3/2} \quad (3)$$

where $E = 10^{53} E_{53}$ erg is the (isotropic) fireball energy, $n = 1 n_1 \text{ cm}^{-3}$ is the ISM number density, and $r = 10^{17} r_{17} \text{ cm}$ is the shell radius. The expansion becomes self-similar at a radius r where two conditions are met: the Lorentz factor $\Gamma_{BM}(r)$ inferred from the self-similar solution is smaller than the initial Lorentz factor Γ , and the width of the shell into which the shocked ISM is compressed in the self-similar solution, $\approx r / 10 \Gamma_{BM}^2(r)$, is larger than the initial fireball shell width cT . The first and second conditions are met for $r > r_T \equiv (17E / 16\pi \Gamma^2 n m_p c^2)^{1/3}$ and $r > r_T \equiv (10 \times 17 E c T / 16\pi n m_p c^2)^{1/4}$ respectively. Thus, the transition to self-similar, external-shock flow occurs at

$$r_e = 5.2 \times 10^{16} \left(\frac{E_{53}}{n_1} \right)^{1/4} \max \left[1.0 T_1^{1/4}, 1.2 \left(\frac{E_{53}}{n_1} \right)^{1/12} \Gamma_{300}^{-2/3} \right] \text{ cm}, \quad (4)$$

where $T = 1 T_1 \text{ s}$.

Internal, mildly-relativistic shocks within the fireball shell result both from variability of the source, at $r_i < r < r_e$, and from the interaction of the fireball with the surrounding gas,

during the transition to a self-similar expansion at $r \sim r_e$, where reverse shocks propagate into the expanding fireball ejecta and decelerate it. From Eq. (4) we infer that for typical fireball parameters the two conditions required for transition to self-similar external shock flow are satisfied at a similar radius, $r_e \approx r_\Gamma \approx r_T$. This implies that significant deceleration of the fireball shell does not take place prior to the transition to self-similar behavior. This, in turn, implies that the reverse shocks propagating into fireball ejecta are only mildly relativistic. Thus, the characteristics of internal shocks due to interaction with surrounding gas are similar to those of internal shocks due to variability on time scale $\sim T$. In the discussion that follows we therefore do not discuss the reverse shocks separately from the internal shocks.

The shock driven into the ISM continuously heats new gas, and produces relativistic electrons that may produce the delayed radiation, “afterglow”, observed on time scales of days to months. As the shock-wave decelerates, the emission shifts to lower frequency with time. Since proton acceleration to high energy takes place only in the internal shocks, $r \leq r_e$ (see §4), we do not discuss further the theory of afterglow emission.

2.2 Afterglow observations

Afterglow observations confirmed, as discussed in the Introduction, the cosmological origin of GRBs, and are consistent with delayed GRB emission being synchrotron radiation of electrons accelerated to high energy in the highly relativistic shock driven by the fireball into its surrounding gas. Since we are interested mainly in the earlier, internal collision phase, of fireball evolution, we do not discuss afterglow observations in detail. We note, however, two implications of afterglow observations which are of importance for the discussion of UHECR production.

The first implication is related to the GRB energy scale. The gamma-ray energy emitted by the three GRBs with measured redshifts in the energy range of 20 keV to 2 MeV (assuming spherical symmetry) is $\approx 10^{52}$ erg, $\approx 0.8 \times 10^{53}$ erg and $\approx 3 \times 10^{53}$ erg for GRB970508 ($z = 0.835$), GRB980703 ($z = 0.966$) and GRB971214 ($z = 3.42$) respectively (here, and throughout the paper, we assume an open universe, $\Omega = 0.2$, $\Lambda = 0$, and $H_0 = 75$ km/s Mpc). This implies that GRBs are not “standard candles,” and that the characteristic gamma-ray energy (luminosity) is $\sim 10^{53}$ erg ($\sim 10^{52}$ erg/s) rather than $\sim 10^{52}$ erg ($\sim 10^{51}$ erg/s) as commonly assumed in the past. Performing a detailed analysis Mao & Mo (1998) find, for example, that the typical luminosity of observed GRBs is $\sim 10^{52}$ erg/s (Note that Mao & Mo use $H_0 = 100$ km/Mpc s and quote luminosities and energies in the 50–300 keV band only).

The second implication relates to the GRB rate. Krumholtz, Thorsett & Harrison [53] (see also [54]) have demonstrated that, based on the data, it is impossible to distinguish between models where the GRB rate per unit comoving volume is independent of redshift, and models where it evolves rapidly, e.g. following star formation rate (previous claims to the contrary were based on the assumption, now known to be invalid, that GRBs are standard candles). Most observed GRBs originate at the redshift range $z \sim 1$ to $z \sim 2$ [53, 54], and the observed GRB rate essentially determines the GRB rate per unit volume at that redshift. The present rate is less well constrained and ranges from $R_{\text{GRB}} \sim 1/\text{Gpc}^3\text{yr}$, assuming the GRB rate evolves rapidly as the star-formation rate, to $R_{\text{GRB}} \sim 10/\text{Gpc}^3\text{yr}$, assuming the GRB rate is independent of redshift. There is some evidence supporting the hypothesis that the GRB rate follows the star

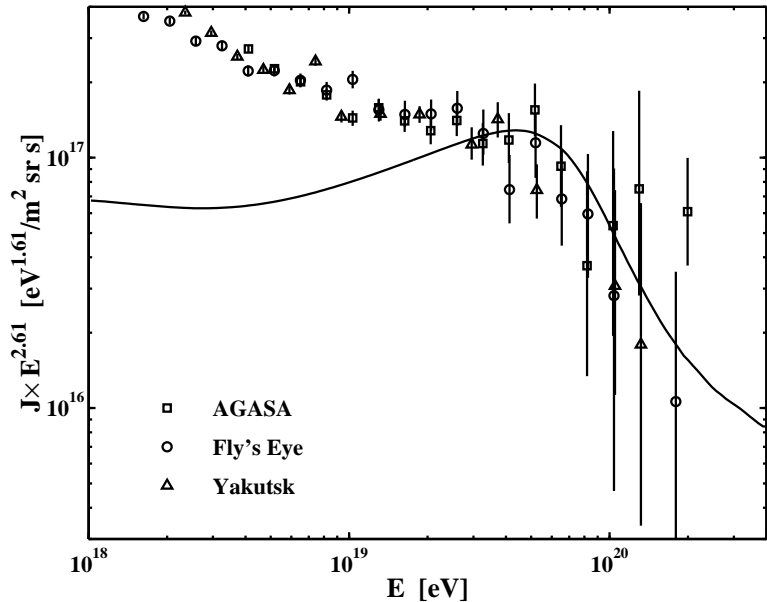


Figure 1: The UHECR flux expected in a cosmological model, where high-energy protons are produced at a rate $E^2 d\dot{n}_{CR}/dE = 0.8 \times 10^{44} \text{ erg/Mpc}^3 \text{ yr}$, compared to the Fly's Eye, Yakutsk and AGASA data. 1σ flux error bars are shown. The highest energy points are derived assuming the detected events (1 for Fly's Eye and Yakutsk, 4 for AGASA) represent a uniform flux over the energy range $10^{20} \text{ eV} - 3 \times 10^{20} \text{ eV}$.

formation rate [55]. The evidence is, however, not yet conclusive.

3 UHECR observations and their implications

Fly's Eye [19] and AGASA [20, 21] results confirm the flattening of the cosmic-ray spectrum at $\sim 10^{19}$ eV, evidence for which existed in previous experiments with weaker statistics [17]. Fly's Eye data is well fitted in the energy range $10^{17.6}$ eV to $10^{19.6}$ eV by a sum of two power laws: A steeper component, with differential number spectrum $J \propto E^{-3.50}$, dominating at lower energy, and a shallower component, $J \propto E^{-2.61}$, dominating at higher energy, $E > 10^{19}$ eV. The flattening of the spectrum, combined with the lack of anisotropy and the evidence for a change in composition from heavy nuclei at low energy to light nuclei (protons) at high energy [17, 19], suggest that an extra-Galactic source of protons dominates the flux at high energy.

In Fig. 1 we compare the UHECR spectrum, reported by the Fly's Eye, the Yakutsk, and the AGASA experiments [19, 18, 21], with that expected from a homogeneous cosmological distribution of sources, each generating a power law differential spectrum of high energy protons $dN/dE \propto E^{-2}$. This spectrum is expected for Fermi shock acceleration [56] (see §4.1 for discussion of the GRB UHECR model). The absolute flux measured at 3×10^{18} eV differs between the various experiments, corresponding to a systematic $\simeq 10\%$ ($\simeq 20\%$) over-estimate of event energies in the AGASA (Yakutsk) experiment compared to the Fly's Eye experiment

(see also [20]). In Fig. 1, the Yakutsk energy normalization is used. For the model calculation, an open universe, $\Omega = 0.2$, $\Lambda = 0$ and $H_0 = 75\text{km/Mpc s}$ were assumed. The calculation is similar to that described in [27]. The generation rate of cosmic-rays (per unit comoving volume) was assumed to evolve rapidly with redshift following the luminosity density evolution of QSOs [57], which is also similar to that describing the evolution of star formation rate [58]: $\dot{n}_{CR}(z) \propto (1+z)^\alpha$ with $\alpha \approx 3$ [59] at low redshift, $z < 1.9$, $\dot{n}_{CR}(z) = \text{Const.}$ for $1.9 < z < 2.7$, and an exponential decay at $z > 2.7$ [60]. The cosmic-ray spectrum at energy $> 10^{19}$ eV is little affected by modifications of the cosmological parameters or of the redshift evolution of cosmic-ray generation rate. This is due to the fact that cosmic-rays at this energy originate from distances shorter than several hundred Mpc. The spectrum and flux at $E > 10^{19}$ eV is mainly determined by the present ($z = 0$) generation rate and spectrum, which in the model shown in Fig. 1 is $E^2(d\dot{n}_{CR}/dE)_{z=0} = 0.8 \times 10^{44}\text{erg/Mpc}^3\text{yr}$.

The suppression of model flux above $\sim 10^{19.7}$ eV, compared to a power-law extrapolation of the flux at low energy, is due to energy loss of high energy protons in interaction with the microwave background, i.e. to the “GZK cutoff” [22]. This is the characteristic signature of cosmological source distribution. It is clear from Fig. 1 that present data does not allow to confirm or rule out the existence of the “cutoff” with high confidence. Nevertheless, some evidence for the cutoff does exist. Both Fly’s Eye and Yakutsk data show a deficit in the number of events detected above $10^{19.7}$ eV, compared to the number expected based on extrapolation of the Fly’s Eye shallower power-law fit for $E < 10^{19.6}$ eV, $J \propto E^{-2.61}$. The deficit is, however, only at a 2σ confidence level [25]. The AGASA data is consistent with Fly’s Eye and Yakutsk results below 10^{20} eV. A discrepancy may be emerging, see Fig. 1, at higher energy, $> 10^{20}$ eV, where the Fly’s Eye and Yakutsk experiments detect 1 event each, and the AGASA experiment detects 6 events for similar exposure (a $\sim 2\sigma$ discrepancy).

We therefore conclude, that a scenario where UHECRs are produced by a cosmological distribution of sources, generating high energy protons at a rate $E^2(d\dot{n}_{CR}/dE)_{z=0} \approx 10^{44}\text{erg/Mpc}^3\text{yr}$, is consistent with the observed flux and spectrum of cosmic-rays in the energy range of 10^{19} eV to 10^{20} eV. The flux predicted by this model above 10^{20} eV is consistent with that measured by the Fly’s Eye and the Yakutsk experiments, while AGASA results suggest a higher flux at this energy. The statistical significance of the discrepancy between the experiments (or between the AGASA results and model prediction above 10^{20} eV) is not high. Clearly, much larger exposure than presently available is required to accurately determine the UHECR spectrum and flux above 5×10^{19} eV.

4 UHECRs from GRB fireballs

4.1 Fermi acceleration in GRBs

In the fireball model, the observed radiation is produced, both during the GRB and the afterglow, by synchrotron emission of shock accelerated electrons. In the region where electrons are accelerated, protons are also expected to be shock accelerated. This is similar to what is thought to occur in supernovae remnant shocks, where synchrotron radiation of accelerated electrons is the likely source of non-thermal X-rays (recent ASCA observations give evidence for acceleration of electrons in the remnant of SN1006 to 10^{14} eV [61]), and where shock accel-

eration of protons is believed to produce cosmic rays with energy extending to $\sim 10^{15}$ eV (see, e.g., [62] for review). Thus, it is likely that protons, as well as electrons, are accelerated to high energy within GRB fireballs. Let us consider the constraints that should be satisfied by the fireball parameters in order to allow acceleration of protons to $\sim 10^{20}$ eV.

We consider proton Fermi acceleration in fireball internal shocks, which take place as the fireball expands over a range of radii $r_i \sim 10^{14}$ cm $\leq r \leq r_e \sim 10^{16}$ cm [cf. Eqs. (1,4)]. As mentioned in §2.1, internal shocks are due to variability of the source, on time scales ranging from the shortest variability time $\Delta t \sim 10$ ms to the wind duration $T \sim 10$ s. In addition, internal shocks arise also due to interaction with ambient gas. The characteristics of the latter internal shocks, which occur at $r \sim r_e$ during the transition to self-similar expansion, are similar to those of internal collisions due to variability on time scale T [see discussion following Eq. (4)]. Internal shocks are, in the wind rest-frame, “mildly relativistic,” i.e. characterized by Lorentz factors $\gamma_i - 1 \sim 1$. We therefore expect results related to particle acceleration in sub-relativistic shocks to be valid for the present scenario. The most restrictive requirement, which rules out the possibility of accelerating particles to energy $\sim 10^{20}$ eV in most astrophysical objects, is that the particle Larmor radius R_L should be smaller than the system size [16]. In our scenario we must apply a more stringent requirement, namely that R_L should be smaller than the largest scale l over which the magnetic field fluctuates, since otherwise Fermi acceleration may not be efficient. We may estimate l as follows. The comoving time, i.e. the time measured in the wind rest frame, is $t = r/\Gamma c$. Thus, regions separated by a comoving distance larger than r/Γ are causally disconnected, and the wind properties fluctuate over comoving length scales up to $l \sim r/\Gamma$. We must therefore require $R_L < r/\Gamma$. A somewhat more stringent requirement is related to the wind expansion. Due to expansion the internal energy is decreasing and therefore available for proton acceleration (as well as for γ -ray production) only over a comoving time $t \sim r/\Gamma c$. The typical Fermi acceleration time is $t_a = f R_L / c \beta^2$, where βc is the Alfvén velocity and $f \sim 1$ [63, 16]. In our scenario $\beta \simeq 1$ leading to the requirement $f R_L < r/\Gamma$. This condition sets a lower limit to the required comoving magnetic field strength. This limit may be stated as a radius independent lower limit to the ratio of magnetic field and electron energy densities [25],

$$\xi_B/\xi_e > 0.02 f^2 \Gamma_{300}^2 E_{p,20}^2 L_{\gamma,52}^{-1}, \quad (5)$$

where $E_p = 10^{20} E_{p,20}$ eV is the accelerated proton energy.

The accelerated proton energy is also limited by energy loss due to synchrotron radiation and interaction with fireball photons. As discussed in §6, the dominant energy loss process is synchrotron cooling. The condition that the synchrotron loss time, $t_{sy} = (6\pi m_p^4 c^3 / \sigma_T m_e^2) E^{-1} B^{-2}$, should be smaller than the acceleration time sets an upper limit to the magnetic field strength. Since the equipartition field decreases with radius, $B_{e,p} \propto r^{-2}$, the upper limit on the magnetic field may be satisfied simultaneously with (5) provided that the internal collisions occur at large enough radius [25],

$$r > 10^{12} f^2 \Gamma_{300}^{-2} E_{p,20}^3 \text{cm}. \quad (6)$$

Since collisions occur at radius $r \approx \Gamma^2 c \Delta t$, the condition (6) is equivalent to a lower limit on Γ

$$\Gamma > 130 f^{1/2} E_{20}^{3/4} \Delta t_{10\text{ms}}^{-1/4}. \quad (7)$$

From Eqs. (5) and (7), we infer that a dissipative ultra-relativistic wind, with luminosity and variability time implied by GRB observations, satisfies the constraints necessary to allow

the acceleration of protons to energy $> 10^{20}$ eV, provided that the wind bulk Lorentz factor is large enough, $\Gamma > 100$, and that the magnetic field is close to equipartition with electrons. The former condition, $\Gamma > 100$, is remarkably similar to that inferred based on the γ -ray spectrum, and $\Gamma \sim 300$ is the “canonical” value assumed in the fireball model. The latter condition, magnetic field close to equipartition, is commonly assumed to be valid in order to account for the observed γ -ray emission [see, e.g., Eq. (2)].

Finally, two points should be clarified. First, it has recently been claimed that ultra-high energy protons would lose most of their energy adiabatically, i.e. due to expansion, before they escape the fireball [41]. This claim is based on the assumptions that internal shocks, and therefore proton acceleration, occur at $r \sim r_i$ only, and that subsequently, $r_i < r < r_e$, the fireball expands adiabatically. Under these assumptions, protons would lose most their energy by the time they escape, at $r \sim r_e$. However, as emphasized both in this section and in §2.1, internal shocks are expected to occur at all radii $r_i < r < r_e$, and in particular at $r \sim r_e$ during the transition to self-similar expansion. Thus, proton acceleration to ultra-high energy is expected to operate at all radii up to $r \sim r_e$, where ultra-high energy particles escape.

Second, it has recently been pointed out in [42] that the conditions at the external shock driven by the fireball into the ambient gas are not likely to allow proton acceleration to ultra-high energy. Although correct, this observation is irrelevant for the acceleration in internal shocks, the scenario considered for UHECR production in GRBs in both [25] and [26].

4.2 UHECR flux and spectrum

We have shown in §3, that the present rate at which energy should be produced as $> 10^{19}$ eV protons by cosmological cosmic-ray sources in order to produce the observed flux is $E^2(dn_{CR}/dE)_{z=0} \approx 10^{44} \text{erg Mpc}^{-3} \text{yr}^{-1}$. This rate is, remarkably, comparable to that produced in γ -rays by cosmological GRBs. The typical GRB γ -ray energy, $E \sim 10^{53}$ erg, and the present ($z = 0$) GRB rate, which is estimated to be in the range of $R_{GRB} = 1/\text{Gpc}^3 \text{yr}$ to $R_{GRB} = 10/\text{Gpc}^3 \text{yr}$ (see discussion in §2.2), implies a present energy generation rate in the range $\sim 10^{44} \text{erg Mpc}^{-3} \text{yr}^{-1}$ to $\sim 10^{45} \text{erg Mpc}^{-3} \text{yr}^{-1}$. In addition, since protons are accelerated in the GRB model to high energy by internal shocks, which in the fireball frame are sub-relativistic, we may expect a generation spectrum $dN/dE \propto E^{-2}$, consistent with UHECR observations (see §3.1).

Thus, GRB fireballs would produce UHECR flux and spectrum consistent with that observed, provided the efficiency with which the wind kinetic energy is converted to γ -rays, and therefore to electron energy, is similar to the efficiency with which it is converted to proton energy, i.e. to UHECRs [25]. There is, however, one additional point which requires consideration [25]. The energy of the most energetic cosmic ray detected by the Fly’s Eye experiment is in excess of 2×10^{20} eV, and that of the most energetic AGASA event is $\sim 2 \times 10^{20}$ eV. On a cosmological scale, the distance traveled by such energetic particles is small: $< 100 \text{Mpc}$ (50Mpc) for the AGASA (Fly’s Eye) event (e.g., [23]). Thus, the detection of these events over a $\sim 5 \text{yr}$ period can be reconciled with the rate of nearby GRBs, ~ 1 per 100yr out to 100Mpc , only if there is a large dispersion, $\geq 100 \text{yr}$, in the arrival time of protons produced in a single burst (This implies that if a direct correlation between high energy CR events and GRBs, as recently suggested in [28], is observed on a $\sim 10 \text{yr}$ time scale, it would be strong evidence *against* a cosmological GRB origin of UHECRs).

The required dispersion is likely to occur due to the combined effects of deflection by random magnetic fields and energy dispersion of the particles [25]. Consider a proton of energy E propagating through a magnetic field of strength B and correlation length λ . As it travels a distance λ , the proton is typically deflected by an angle $\alpha \sim \lambda/R_L$, where $R_L = E/eB$ is the Larmor radius. The typical deflection angle for propagation over a distance D is $\theta_s \sim (D/\lambda)^{1/2}\lambda/R_L$. This deflection results in a time delay, compared to propagation along a straight line,

$$\tau(E, D) \approx \theta_s^2 D / 4c \approx 2 \times 10^5 E_{20}^{-2} D_{100}^2 \lambda_{\text{Mpc}} B_{\text{nG}}^2 \text{ yr}, \quad (8)$$

where $D = 100 D_{100} \text{Mpc}$, $\lambda = 1 \lambda_{\text{Mpc}} \text{ Mpc}$ and $B = 10^{-9} B_{\text{nG}} \text{ G}$. Here, we have chosen numerical values corresponding to the current upper bound on the inter-galactic magnetic field, $B\lambda^{1/2} \leq 10^{-9} \text{ G Mpc}^{1/2}$ [64]. The random energy loss UHECRs suffer as they propagate, owing to the production of pions, implies that at any distance from the observer there is some finite spread in the energies of UHECRs that are observed with a given fixed energy. For protons with energies $> 10^{20} \text{ eV}$ the fractional RMS energy spread is of order unity over propagation distances in the range $10 - 100 \text{ Mpc}$ (e.g. [23]). Since the time delay is sensitive to the particle energy, this implies that the spread in arrival time of UHECRs with given observed energy is comparable to the average time delay at that energy $\tau(E, D)$ (This result has been confirmed by numerical calculations in [65]). Thus, the required time spread, $\tau > 100 \text{ yr}$, is consistent with the upper bound, $\tau < 2 \times 10^5 \text{ yr}$, implied by the present upper bound to the inter-galactic magnetic field.

5 GRB model predictions for UHECR experiments

5.1 The Number and Spectra of Bright Sources

The initial proton energy, necessary to have an observed energy E , increases with source distance due to propagation energy losses. The rapid increase of the initial energy after it exceeds, due to electron-positron production, the threshold for pion production effectively introduces a cutoff distance, $D_c(E)$, beyond which sources do not contribute to the flux above E . The function $D_c(E)$ is shown in Fig. 2 (taken from [29]). Since $D_c(E)$ is a decreasing function of E , for a given number density of sources there is a critical energy E_c , above which only one source (on average) contributes to the flux. In the GRB model E_c depends on the product of the burst rate R_{GRB} and the time delay. The number of sources contributing, on average, to the flux at energy E is [29]

$$N(E) = \frac{4\pi}{5} R_{\text{GRB}} D_c(E)^3 \tau [E, D_c(E)] \quad , \quad (9)$$

and the average intensity resulting from all sources is

$$J(E) = \frac{1}{4\pi} R_{\text{GRB}} \frac{dn_p}{dE} D_c(E) \quad , \quad (10)$$

where dn_p/dE is the number per unit energy of protons produced on average by a single burst (this is the formal definition of $D_c(E)$). The critical energy E_c is given by

$$\frac{4\pi}{5} R_{\text{GRB}} D_c(E_c)^3 \tau [E_c, D_c(E_c)] = 1 \quad . \quad (11)$$

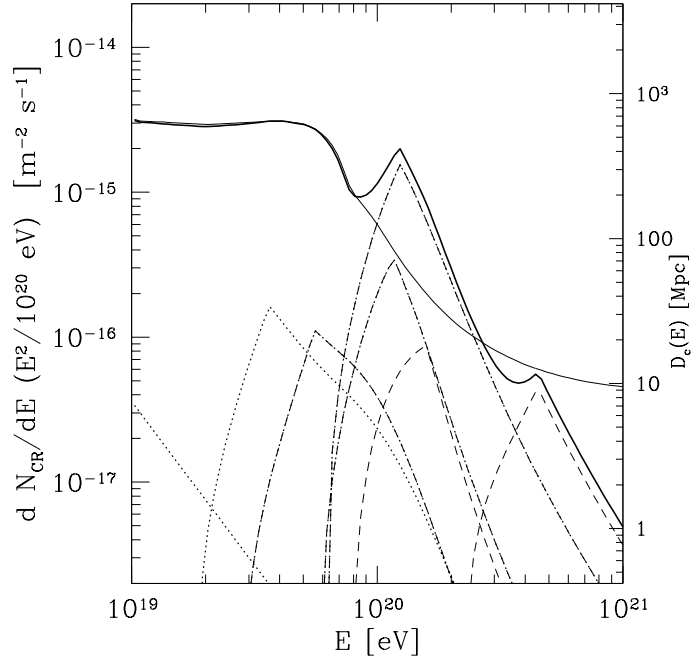


Figure 2: Results of a Monte-Carlo realization of the bursting sources model, with $E_c = 1.4 \times 10^{20}$ eV: Thick solid line- overall spectrum in the realization; Thin solid line- average spectrum, this curve also gives $D_c(E)$; Dotted lines- spectra of brightest sources at different energies.

E_c , the energy beyond which a single source contributes on average to the flux, depends on the unknown properties of the intergalactic magnetic field, $\tau \propto B^2\lambda$. However, the rapid decrease of $D_c(E)$ with energy near 10^{20} eV, see Fig. 2, implies that E_c is only weakly dependent on the value of $B^2\lambda$. In The GRB model, the product $R_{GRB}\tau(D = 100\text{Mpc}, E = 10^{20}\text{eV})$ is approximately limited to the range 10^{-6} Mpc^{-3} to 10^{-3} Mpc^{-3} (The lower limit is set by the requirement that at least a few GRB sources be present at $D < 100$ Mpc, and the upper limit by the Faraday rotation bound $B\lambda^{1/2} \leq 10^{-9}\text{G Mpc}^{1/2}$ [64] and $R_{GRB} \leq 10/\text{Gpc}^3\text{yr}$). The corresponding range of values of E_c is $10^{20}\text{eV} \leq E_c < 3 \times 10^{20}\text{eV}$.

Fig. 2 presents the flux obtained in one realization of a Monte-Carlo simulation described by Miralda-Escudé & Waxman [29] of the total number of UHECRs received from GRBs at some fixed time. For each realization the positions (distances from Earth) and times at which cosmological GRBs occurred were randomly drawn, assuming, an intrinsic proton generation spectrum $dN_p/dE_p \propto E_p^{-2}$, and $E_c = 1.4 \times 10^{20}\text{eV}$. Most of the realizations gave an overall spectrum similar to that obtained in the realization of Fig. 2 when the brightest source of this realization (dominating at 10^{20}eV) is not included. At $E < E_c$, the number of sources contributing to the flux is very large, and the overall UHECR flux received at any given time is near the average (the average flux is that obtained when the UHECR emissivity is spatially uniform and time independent). At $E > E_c$, the flux will generally be much lower than the average, because there will be no burst within a distance $D_c(E)$ having taken place sufficiently recently. There is, however, a significant probability to observe one source with a flux higher

than the average. A source similar to the brightest one in Fig. 2 appears $\sim 5\%$ of the time.

At any fixed time a given burst is observed in UHECRs only over a narrow range of energy, because if a burst is currently observed at some energy E then UHECRs of much lower energy from this burst have not yet arrived, while higher energy UHECRs reached us mostly in the past. As mentioned above, for energies above the pion production threshold, $E \sim 5 \times 10^{19}$ eV, the dispersion in arrival times of UHECRs with fixed observed energy is comparable to the average delay at that energy. This implies that the spectral width ΔE of the source at a given time is of order the average observed energy, $\Delta E \sim E$. Thus, bursting UHECR sources should have narrowly peaked energy spectra, and the brightest sources should be different at different energies. For steady state sources, on the other hand, the brightest source at high energies should also be the brightest one at low energies, its fractional contribution to the overall flux decreasing to low energy only as $D_c(E)^{-1}$. A detailed numerical analysis of the time dependent energy spectrum of bursting sources is given in [66, 67].

5.2 Spectra of Sources at $E < 4 \times 10^{19}$ eV

The detection of UHECRs above 10^{20} eV imply that the brightest sources must lie at distances smaller than 100 Mpc. UHECRs with $E \leq 4 \times 10^{19}$ eV from such bright sources will suffer energy loss only by pair production, because at $E < 5 \times 10^{19}$ eV the mean-free-path for pion production interaction (in which the fractional energy loss is $\sim 10\%$) is larger than 1 Gpc. Furthermore, the energy loss due to pair production over 100 Mpc propagation is only $\sim 5\%$.

In the case where the typical displacement of the UHECRs due to deflections by intergalactic magnetic fields is much smaller than the correlation length, $\lambda \gg D\theta_s(D, E) \simeq D(D/\lambda)^{1/2}\lambda/R_L$, all the UHECRs that arrive at the observer are essentially deflected by the same magnetic field structures, and the absence of random energy loss during propagation implies that all rays with a fixed observed energy would reach the observer with exactly the same direction and time delay. At a fixed time, therefore, the source would appear mono-energetic and point-like. In reality, energy loss due to pair production results in a finite but small spectral and angular width, $\Delta E/E \sim \delta\theta/\theta_s \leq 1\%$ [30].

In the case where the typical displacement of the UHECRs is much larger than the correlation length, $\lambda \ll D\theta_s(D, E)$, the deflection of different UHECRs arriving at the observer are essentially independent. Even in the absence of any energy loss there are many paths from the source to the observer for UHECRs of fixed energy E that are emitted from the source at an angle $\theta \leq \theta_s$ relative to the source-observer line of sight. Along each of the paths, UHECRs are deflected by independent magnetic field structures. Thus, the source angular size would be of order θ_s and the spread in arrival times would be comparable to the characteristic delay τ , leading to $\Delta E/E \sim 1$ even when there are no random energy losses. The observed spectral shape of a nearby ($D < 100$ Mpc) bursting source of UHECRs at $E < 4 \times 10^{19}$ eV was derived for the case $\lambda \ll D\theta_s(D, E)$ in [30], and is given by

$$\frac{dN}{dE} \propto \sum_{n=1}^{\infty} (-1)^{n+1} n^2 \exp\left[-\frac{2n^2\pi^2 E^2}{E_0^2(t, D)}\right] \quad , \quad (12)$$

where $E_0(t, D) = De(2B^2\lambda/3ct)^{1/2}$. For this spectrum, the ratio of the RMS UHECR energy spread to the average energy is 30%

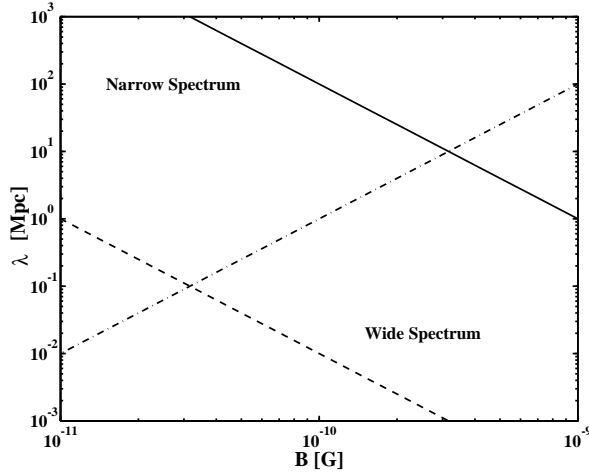


Figure 3: The line $\theta_s D = \lambda$ for a source at 30Mpc distance observed at energy $E \simeq 10^{19}$ eV (dot-dash line), shown with the Faraday rotation upper limit $B\lambda^{1/2} \leq 10^{-9}$ G Mpc $^{1/2}$ (solid line), and with the lower limit $B\lambda^{1/2} \geq 10^{-11}$ G Mpc $^{1/2}$ required in the GRB model.

Fig. 3 shows the line $\theta_s D = \lambda$ in the $B - \lambda$ plane, for a source at a distance $D = 30$ Mpc observed at energy $E \simeq 10^{19}$ eV. Since the $\theta_s D = \lambda$ line divides the allowed region in the plane at $\lambda \sim 1$ Mpc, measuring the spectral width of bright sources would allow to determine if the field correlation length is much larger, much smaller, or comparable to 1Mpc.

6 High energy Neutrinos

6.1 Neutrino production

6.1.1 Neutrinos at energies $\sim 10^{14}$ eV

Protons accelerated in the fireball to high energy lose energy through photo-meson interaction with fireball photons. The decay of charged pions produced in this interaction, $\pi^+ \rightarrow \mu^+ + \nu_\mu \rightarrow e^+ + \nu_e + \bar{\nu}_\mu + \nu_\mu$, results in the production of high energy neutrinos. The neutrino spectrum is determined by the observed gamma-ray spectrum, which is well described by a broken power-law, $dN_\gamma/dE_\gamma \propto E_\gamma^{-\beta}$ with different values of β at low and high energy [68]. The observed break energy (where β changes) is typically $E_\gamma^b \sim 1$ MeV, with $\beta \simeq 1$ at energies below the break and $\beta \simeq 2$ above the break. The interaction of protons accelerated to a power-law distribution, $dN_p/dE_p \propto E_p^{-2}$, with GRB photons results in a broken power law neutrino spectrum [34], $dN_\nu/dE_\nu \propto E_\nu^{-\beta}$ with $\beta = 1$ for $E_\nu < E_\nu^b$, and $\beta = 2$ for $E_\nu > E_\nu^b$. The neutrino break energy E_ν^b is fixed by the threshold energy of protons for photo-production in interaction with the dominant ~ 1 MeV photons in the GRB,

$$E_\nu^b \approx 5 \times 10^{14} \Gamma_{300}^2 (E_\gamma^b / 1\text{MeV})^{-1} \text{eV}. \quad (13)$$

The normalization of the flux is determined by the efficiency of pion production. As shown in [34], the fraction of energy lost to pion production by protons producing the neutrino flux

above the break, E_ν^b , is essentially independent of energy and is given by

$$f_\pi \approx 0.2 \frac{L_{\gamma,52}}{(E_\gamma^b/1\text{MeV})\Gamma_{300}^4 \Delta t_{10\text{ms}}}. \quad (14)$$

Thus, acceleration of protons to high energy in internal fireball shocks would lead to conversion of a significant fraction of proton energy to high energy neutrinos.

If GRBs are the sources of UHECRS, then using Eq. (14) and the UHECR generation rate implied by observations, the expected GRB neutrino flux is [69]

$$\begin{aligned} E_\nu^2 \Phi_{\nu_\mu} &\approx E_\nu^2 \Phi_{\bar{\nu}_\mu} \approx E_\nu^2 \Phi_{\nu_e} \\ &\approx 1.5 \times 10^{-9} \left(\frac{f_\pi}{0.2} \right) \min\{1, E_\nu/E_\nu^b\} \text{GeV cm}^{-2} \text{s}^{-1} \text{sr}^{-1}. \end{aligned} \quad (15)$$

The GRB neutrino flux can be estimated directly from the observed gamma-ray fluence. The Burst and Transient Source Experiment (BATSE) measures the GRB fluence F_γ over two decades of photon energy, $\sim 0.02\text{MeV}$ to $\sim 2\text{MeV}$, corresponding to a decade of radiating electron energy (the electron synchrotron frequency is proportional to the square of the electron Lorentz factor). If electrons carry a fraction f_e of the energy carried by protons, then the muon neutrino fluence of a single burst is $E_\nu^2 dN_\nu/dE_\nu \approx 0.25(f_\pi/f_e)F_\gamma/\ln(10)$. The average neutrino flux per unit time and solid angle is obtained by multiplying the single burst fluence with the GRB rate per solid angle, $\approx 10^3$ bursts per year over 4π sr. Using the average burst fluence $F_\gamma = 10^{-5}\text{erg/cm}^2$, we obtain a muon neutrino flux $E_\nu^2 \Phi_\nu \approx 3 \times 10^{-9}(f_\pi/f_e)\text{GeV/cm}^2 \text{s sr}$. Thus, the neutrino flux estimated directly from the gamma-ray fluence agrees with the estimate (15) based on the cosmic-ray production rate.

6.1.2 Neutrinos at high energy $> 10^{16}$ eV

The neutrino spectrum (15) is modified at high energy, where neutrinos are produced by the decay of muons and pions whose life time $\tau_{\mu,\pi}$ exceeds the characteristic time for energy loss due to adiabatic expansion and synchrotron emission [34, 70, 69]. The synchrotron loss time is determined by the energy density of the magnetic field in the wind rest frame. For the characteristic parameters of a GRB wind, the muon energy for which the adiabatic energy loss time equals the muon life time, E_μ^a , is comparable to the energy E_μ^s at which the life time equals the synchrotron loss time, τ_μ^s . For pions, $E_\pi^a > E_\pi^s$. This, and the fact that the adiabatic loss time is independent of energy and the synchrotron loss time is inversely proportional to energy, imply that synchrotron losses are the dominant effect suppressing the flux at high energy. The energy above which synchrotron losses suppress the neutrino flux is

$$\frac{E_{\nu_\mu(\bar{\nu}_\mu,\nu_e)}^s}{E_\nu^b} \approx (\xi_B L_{\gamma,52}/\xi_e)^{-1/2} \Gamma_{300}^2 \Delta t_{10\text{ms}} (E_\gamma^b/1\text{MeV}) \times \begin{cases} 10, & \text{for } \bar{\nu}_\mu, \nu_e; \\ 100, & \text{for } \nu_\mu. \end{cases} \quad (16)$$

We note, that the results presented above were derived using the “ Δ -approximation,” i.e. assuming that photo-meson interactions are dominated by the contribution of the Δ -resonance. It has recently been shown [71], that for photon spectra harder than $dN_\gamma/dE_\gamma \propto E_\gamma^{-2}$, the contribution of non-resonant interactions may be important. Since in order to interact with the

hard part of the photon spectrum, $E_\gamma < E_\nu^b$, the proton energy must exceed the energy at which neutrinos of energy E_ν^b are produced, significant modification of the Δ -approximation results is expected only for $E_\nu \gg E_\nu^b$, where the neutrino flux is strongly suppressed by synchrotron losses.

So far, we have discussed neutrino production in internal shocks due to variability on the shortest time scale, $\Delta t \sim 10$ ms. Internal collisions due to variability on longer time scales, $\Delta t < \delta t < T$, are less efficient in producing neutrinos, $f_\pi \propto \delta t^{-1}$ [cf. Eq. (14)], since the radiation energy density is lower at larger collision radii. However, at larger radii synchrotron losses cut off the spectrum at higher energy, $E^s(\delta t) \propto \delta t$ [cf. Eq. (16)]. Collisions at large radii therefore result in extension of the neutrino spectrum of Eq. (15) to higher energy, beyond the cutoff energy Eq. (16),

$$E_\nu^2 \Phi_\nu \propto E_\nu^{-1}, \quad E_\nu > E_\nu^s. \quad (17)$$

The neutrino flux from GRBs is small above 10^{19} eV, and a neutrino flux comparable to the γ -ray flux is expected only below $\sim 10^{17}$ eV, in agreement with the results of ref. [70]. Our result is not in agreement, however, with that of ref. [72], where a much higher flux at $\sim 10^{19}$ eV is obtained based on the equations of ref. [34], which are the same equations as used here³. Finally, we note that, contrary to the claim in [70], there is no contradiction between production of high-energy protons above $\sim 3 \times 10^{20}$ eV and a break in the neutrino spectrum at $\sim 10^{16}$ eV [cf. Eqs. (5,7,16)].

6.2 Implications

The high energy neutrinos predicted in the dissipative wind model of GRBs may be observed by detecting the Cerenkov light emitted by high energy muons produced by neutrino interactions below a detector on the surface of the Earth (see [73] for a recent review). The probability $P_{\nu\mu}$ that a neutrino would produce a high energy muon in the detector is approximately given by the ratio of the high energy muon range to the neutrino mean free path. At the high energy we are considering, $P_{\nu\mu} \simeq 10^{-6}(\epsilon_\nu/1\text{TeV})$ [73]. Using Eq. (15), this implies a detection rate of ~ 20 neutrino induced muons per year for a 1 km^2 detector (over 4π sr). As discussed in [34], one may look for neutrino events in angular coincidence, on degree scale, and temporal coincidence, on time scale of seconds, with GRBs. Several authors [74] have recently emphasized the effect on muon detection rate of neutrino absorption in the Earth. This effect is not large for GRB neutrinos, since most of the signal comes from neutrinos of energy $\sim 10^{14}$ eV. At this energy, the flux of upward moving muons is reduced due to absorption by 36% [74], and the total (4π sr) flux is reduced by only 18%.

Detection of neutrinos from GRBs could be used to test the simultaneity of neutrino and photon arrival to an accuracy of ~ 1 s (~ 1 ms for short bursts), checking the assumption of special relativity that photons and neutrinos have the same limiting speed [The time delay for neutrino of energy 10^{14} eV with mass m_ν traveling 100 Mpc is only $\sim 10^{-11}(m_\nu/10\text{ eV})^2$ s]. These observations would also test the weak equivalence principle, according to which photons

³The parameters chosen in [72] are $L_\gamma = 10^{50}\text{erg/s}$, $\Delta t = 10\text{s}$, and $\Gamma = 100$. Using equation (4) of ref. [34], which is the same as Eq. (14) of the present paper, we obtain for these parameters $f_\pi = 1.6 \times 10^{-4}$, while the author of [72] obtains, using the same equation, $f_\pi = 0.03$.

and neutrinos should suffer the same time delay as they pass through a gravitational potential. With 1 s accuracy, a burst at 100 Mpc would reveal a fractional difference in limiting speed of 10^{-16} , and a fractional difference in gravitational time delay of order 10^{-6} (considering the Galactic potential alone). Previous applications of these ideas to supernova 1987A (see [75] for review), where simultaneity could be checked only to an accuracy of order several hours, yielded much weaker upper limits: of order 10^{-8} and 10^{-2} for fractional differences in the limiting speed [76] and time delay [77] respectively.

The model discussed above predicts the production of high energy muon and electron neutrinos with a 2:1 ratio. If vacuum neutrino oscillations occur in nature, then neutrinos that get here should be almost equally distributed between flavors for which the mixing is strong. In fact, if the atmospheric neutrino anomaly has the explanation it is usually given, oscillation to ν_τ 's with mass ~ 0.1 eV [78], then one should detect equal numbers of ν_μ 's and ν_τ 's. Upgoing τ 's, rather than μ 's, would be a distinctive signature of such oscillations. Since ν_τ 's are not expected to be produced in the fireball, looking for τ 's would be an “appearance experiment” (ν_τ 's may be produced by photo-production of charmed mesons; However, the high photon threshold, ~ 50 GeV, and low cross-section, $\sim 1\mu\text{b}$ [79], for such reactions imply that the ratio of charmed meson to pion production is $\sim 10^{-4}$). To allow flavor change, the difference in squared neutrino masses, Δm^2 , should exceed a minimum value proportional to the ratio of source distance and neutrino energy [75]. A burst at 100 Mpc producing 10^{14} eV neutrinos can test for $\Delta m^2 \geq 10^{-16}\text{eV}^2$, 5 orders of magnitude more sensitive than solar neutrinos. Note, that due to the finite pion life time, flavor mixing would be caused by de-coherence, rather than by real oscillations, for neutrinos with masses > 0.1 eV.

7 Summary

Afterglow observations confirmed the cosmological origin of GRBs and provide support for the fireball model (§1,§2). In this model, observed radiation is produced by synchrotron emission of shock accelerated electrons. We have shown, that in the region where electrons are accelerated protons can be accelerated to ultra-high energy (§4.1). Acceleration to $> 10^{20}$ eV is possible provided that the fireball bulk Lorentz factor is large enough, $\Gamma > 100$, and that the magnetic field is close to equipartition with electrons. The former condition, $\Gamma > 100$, is remarkably similar to that inferred based on γ -ray spectra, and $\Gamma \sim 300$ is the “canonical” value assumed in the fireball model. The latter condition is commonly assumed to be valid in order to account for observed γ -ray emission.

Observed UHECR flux and spectrum are consistent with a model where UHECRs are protons accelerated to high energy in GRB fireballs, provided the efficiency with which fireball kinetic energy is converted to γ -rays, and therefore to accelerated electron energy, is similar to the efficiency with which it is converted to accelerated proton energy (§3,§4.2).

The GRB model for UHECR production has several unique predictions (§5). In particular, a critical energy is predicted to exist, $10^{20}\text{eV} \leq E_c < 3 \times 10^{20}\text{eV}$, above which a few sources produce most of the UHECR flux, and the observed spectra of these sources is predicted to be narrow, $\Delta E/E \sim 1$: the bright sources at high energy should be absent in UHECRs of much lower energy, since particles take longer to arrive the lower their energy. Recently, the AGASA

experiment reported the presence of 3 pairs of UHECRs with angular separations (within each pair) $\leq 2.5^\circ$, roughly consistent with the measurement error, among a total of 36 UHECRs with $E \geq 4 \times 10^{19}$ eV [80]. The two highest energy AGASA events were in these pairs. Given the total solid angle observed by the experiment, $\sim 2\pi\text{sr}$, the probability to have found 3 pairs by chance is $\sim 3\%$; and, given that three pairs were found, the probability that the two highest energy events are among the three pairs by chance is 2.4%. Therefore, this observation favors the bursting source model, although more data are needed to confirm it. Testing the above predictions of the fireball model for UHECR production would require an exposure 10 times larger than that of present experiments. Such increase is expected to be provided by the planned HiRes [31] and Auger [32] detectors.

A natural consequence of proton acceleration in fireball shocks is the conversion of a large fraction, $\geq 10\%$, of the fireball energy to a burst of $\sim 10^{14}$ eV neutrinos by photo-meson production (§6.1). Large area, $\sim 1\text{km}^2$, high-energy neutrino telescopes, which are being constructed to detect cosmologically distant neutrino sources, would observe several tens of events per year correlated with GRBs, and test for neutrino properties (e.g. flavor oscillations, for which upward moving τ 's would be a unique signature, and coupling to gravity) with an accuracy many orders of magnitude better than is currently possible (§6.2).

References

- [1] Fishman, G. J. & Meegan, C. A., *ARA&A* **33**, 415 (1995).
- [2] C. A. Meegan *et al.*, *Nature* **355**, 143 (1992); B. Paczyński, *Nature* **355**, 521 (1992).
- [3] Mészáros, P., in Proc. 17th Texas Conf. Relativistic Astrophysics, *Annals Ny. Acad. Sci.* No. 759 (NY Acad. Sci., NY 1995); Piran, T., in *Unsolved Problems In Astrophysics*, eds. J. N. Bahcall and J. P. Ostriker, 343-377 (Princeton, 1996).
- [4] Costa, E. *et al.*, *Nature* **387**, 783 (1997).
- [5] van Paradijs, J. *et al.*, *Nature* **386**, 686 (1997).
- [6] Frail, D. A. *et al.*, *Nature* **389**, 261 (1997).
- [7] Metzger, M. R. *et al.* 1997, *Nature*, 387, 879.
- [8] Bloom, J. S., Sigurdsson, S., & Pols, O. R., *MNRAS* in press (astro-ph/9805222) (1998).
- [9] Djorgovski, S. G. *et al.*, *Ap. J.*, in press (astro-ph/9808188) (1998).
- [10] Kulkarni, S. R. *et al.*, *Nature* **393**, 35 (1998).
- [11] Paczyński, B. & Rhoads, J., *Ap. J.* **418**, L5 (1993); Katz, J. I., *Ap. J.* **432**, L107 (1994); Mészáros, P. & Rees, M., *Ap. J.* **476**, 232 (1997); Vietri, M., *Ap. J.* **478**, L9 (1997).

- [12] Waxman, E., Ap. J. **485**, L5 (1997); Wijers, R. A. M. J., Rees, M. J. & Mészáros, P., MNRAS **288**, L51 (1997); Sari, R., Piran , T., & Narayan, R., Ap. J. **497**, L17 (1998). Wijers, R. A. M. J., & Galama, T.J., astro-ph/98050341 (1998); Granot, J, Piran, T. & Sari, R., astro-ph/9808007 (1998).
- [13] Goodman, J., New Astronomy **2**, 449 (1997).
- [14] Waxman, E., Kulkarni, S., Frail, D., Ap. J. **497**, 288 (1998).
- [15] Cronin, J. W., in Unsolved Problems In Astrophysics, eds. J. N. Bahcall and J. P. Ostriker (Princeton, 1996).
- [16] A. M. Hillas, ARA&A **22**, 425 (1984).
- [17] Watson, A. A., Nucl. Phys. B (Proc. Suppl.) **22B**, 116 (1991).
- [18] N.N. Efimov *et al.*, in *Proceedings of the International Symposium on Astrophysical Aspects of the Most Energetic Cosmic-Rays*, edited by M. Nagano and F. Takahara (World Scientific, Singapore, 1991), p. 20.
- [19] Bird, D. J., *et al.*, Phys. Rev. Lett. **71**, 3401 (1993); Bird, D. J., *et al.*, Ap. J. **424**, 491 (1994).
- [20] Hayashida, N. *et al.*, Phys. Rev. Lett. **73**, 3491 (1994); Yoshida, S., *et al.*, Astropar. Phys. **3**, 151 (1995).
- [21] Takeda, M. *et al.*, Phys. Rev. Lett. **81**, 1163 (1998).
- [22] Greisen, K., Phys. Rev. Lett. **16**, 748 (1966); Zatsepin, G. T., & Kuzmin, V. A., JETP lett., **4**, 78 (1966).
- [23] Aharonian, F. A., & Cronin, J. W., Phys. Rev. D **50**, 1892 (1994).
- [24] Sigl, G., Schramm, D. N., & P. Bhattacharjee, Astropar. Phys., **2**, 401 (1994); Elbert, J. W., & Sommers, P., Ap. J. **441**, 151 (1995).
- [25] Waxman, E., Phys. Rev. Lett. **75**, 386 (1995).
- [26] Vietri, M., Ap. J. **453**, 883 (1995).
- [27] Waxman, E., Ap. J. **452**, L1 (1995).
- [28] Milgrom, M. & Usov, V., Ap. J. **449**, L37 (1995).
- [29] Miralda-Escudé, J. & Waxman, E., Ap. J. **462**, L59 (1996).
- [30] Waxman, E. & Miralda-Escudé, J., Ap. J. **472**, L89 (1996).
- [31] Corbató, S. C. *et al.*, Nuc. Phys. **28B** (Proc. Suppl.), 36 (1992); see also <http://www.physics.adelaide.edu.au/astrophysics/FlyEye.html>

- [32] Cronin, J. W., these proceedings; Cronin, J. W., Nucl. Phys. B (Proc. Suppl.) **28B**, 213 (1992); Watson, A. A., in Nuclear and Particle Phys. 1993, eds. MacGregor, I. J. D. & Doyle, A. T. (Inst. Phys. Conf. Ser. **133**) (Bristol:IoP), 135; see also <http://www.auger.org/>
- [33] Teshima, M. *et al.*, Nuc. Phys. **28B** (Proc. Suppl.), 169 (1992); see also <http://www-ta.icrr.u-tokyo.ac.jp/>
- [34] Waxman, E., & Bahcall, J. N., Phys. Rev. Lett. **78**, 2292 (1997).
- [35] Barwick, S., these proceedings; see also <http://amanda.berkeley.edu/km3/>
- [36] Lowder, D. M. *et al.* 1991, Nature 353, 331; Halzen, F. 1997, Summary talk of The XXXIIInd Rencontre de Moriond, Les Arcs, France 1997 (astro-ph/9703004).
- [37] see <http://antares.in2p3.fr/antares/antares.html>
- [38] see <http://abyss.hepl.uoa.ariadne-t.gr>
- [39] Rees, M. J., these proceedings
- [40] Watson, A. A., these proceedings
- [41] Rachen, J. P., & Mészáros, P., Proc. 4th Huntsville Symposium on GRBs, 1998 (AIP Conf. Proc. **428**, Gamma Ray Bursts), p. 776
- [42] Gallant, Y. A., & Achterberg, A., submitted to MNRAS (astro-ph/9812316)
- [43] Bhat, P. N., *et al.*, Nature **359**, 217 (1992); Fishman, G. J., *et al.*, Ap. J. Supp. **92**, 229 (1994).
- [44] Paczyński, B., Ap. J. **308**, L43 (1986); Goodman, J., Ap. J. **308**, L47 (1986);
- [45] Krolik, J. H. & Pier, E. A., Ap. J. **373**, 277 (1991); Baring, M., Ap. J. **418**, 391 (1993).
- [46] Paczyński, B., Ap. J. **363**, 218 (1990); Shemi, A., & Piran, T., Ap. J. **365**, L55 (1990).
- [47] Rees, M. & Mészáros, P., MNRAS **258**, 41P (1992).
- [48] Narayan, R., Paczyński, B., & Piran, T., Ap. J. **395**, L83 (1992); Paczyński, B. & Xu, G., Ap. J. **427**, 708 (1994); Mészáros, P., & Rees, M., MNRAS **269**, 41P (1994).
- [49] Woods, E. & Loeb, A., Ap. J. **453**, 583 (1995).
- [50] Sari, R., & Piran, T., Ap. J. **485**, 270 (1997).
- [51] Walker, K. C. & Schaefer, B. E., submitted to Ap. J. (astro-ph/9810271).
- [52] Blandford, R. D., & McKee, C. F., Phys. Fluids **19**, 1130 (1976).
- [53] Krumholz, M., Thorsett, S. E., & Harrison, F. A., Ap. J. **506**, L81 (1998).

- [54] Hogg, D. W. & Fruchter, A. S., submitted to Ap. J. (astro-ph/9807262).
- [55] Kulkarni, S. R., *et al.*, Nature **393**, 35 (1998); Metzger, M., *et al.*, IAUC 6676 (1997); Fruchter, A. S., *et al.*, Proc. 4th Huntsville Symposium on GRBs, 1998 (AIP Conf. Proc. **428**, Gamma Ray Bursts).
- [56] Axford, W. I., Leer, E., & Skadron, G., Proc. 15th Int. Conf. Cosmic Rays, Plovdiv, Bulgaria (1977); Bell, A. R., MNRAS **182**, 147 (1978); Blandford, R. D., & Ostriker, J. P., Ap. J. **221**, L229 (1978).
- [57] Boyle, B. J. & Terlevich, R. J., MNRAS **293**, L49 (1998).
- [58] Lilly, S. J. , Le Fevre, O., Hammer F., & Crampton, D., Ap. J. **460**, L1 (1996); Madau, P., *et al.* MNRAS **283**, 1388 (1996).
- [59] Hewett, P. C., Foltz, C. B. & Chaffee, F., Ap. J. **406**, 43 (1993).
- [60] Schmidt, M., Schneider, D. P., & Gunn, J. E., Astron. J. **110**, 68 (1995).
- [61] Koyama, K. *et al.*, Nature **378**, 255 (1995).
- [62] Blandford, R., & Eichler, D., Phys. Rep. **154**, 1 (1987).
- [63] R. M. Kulsrud, in *Particle Acceleration Mechanisms in Astrophysics*, eds. J. Arons, C. Max, and C. McKee (AIP 56, NY 1979).
- [64] Kronberg, P. P., Rep. Prog. Phys. **57**, 325 (1994); Vallee, J. P., Ap. J. **360**, 1 (1990).
- [65] Waxman, E., & Coppi, P., Ap. J. **464**, L75 (1996).
- [66] Sigl, G., Lemoine, M. & Olinto, A. V., Phys. Rev. **D56**, 4470 (1997).
- [67] Lemoine, M., Sigl, G., Olinto, A. V. & Schramm, D. N., Ap. J. **486**, L115 (1997).
- [68] Band, D., *et al.*, Ap. J. **413**, 281 (1993).
- [69] Waxman, E., & Bahcall, J. N., Phys. Rev. **D59**, 023002 (1999).
- [70] Rachen, J. P., & Mészáros, P., Submitted to Phys. Rev. D (1998) (astro-ph/9802280).
- [71] Muecke, A. *et al.*, submitted to Ap. J. (astro-ph/9808279).
- [72] Vietri, M., Phys. Rev. Lett. **80**, 3690 (1998).
- [73] Gaisser, T. K., Halzen, F., & Stanev, T., Phys. Rep. **258**, 173 (1995).
- [74] Gandhi, R., Quigg, C., Reno, M., & Sarcevic, I., Phys. Rev. **D58**, 093009 (1998); Kwiecinski, J., Martin, A. D., Stasto, A. submitted to Phys. Rev. D (astro-ph/9812262).
- [75] Bahcall, J. N., *Neutrino Astrophysics*, Cambridge University Press (NY 1989).

- [76] Stodolsky, L., Phys. Lett. **B201**, 353 (1988).
- [77] Krauss, L. M., & Tremaine, S., Phys. Rev. Lett. **60**, 176 (1988); Longo, M. J., Phys. Rev. Lett. **60**, 173 (1988).
- [78] Fukuda, Y., *et al.*, Phys. Lett. **B335**, 237 (1994); Casper, D., *et al.*, Phys. Rev. Lett. **66**, 2561 (1991); Fogli, G. L., & Lisi, E., Phys. Rev. **D52**, 2775 (1995).
- [79] Anjos, J. C., *et al.*, Phys. Rev. Lett. **62**, 513 (1989).
- [80] Hayashida, N., *et al.* Phys. Rev. Lett. **77**, 1000 (1996).